Supplementary Information: Advances in the Projected Forces and Momenta Decoherence Method for Attosecond Nonadiabatic Molecular Dynamics

Gilbert Grell[a†], Joachim Galiana[b], Stefano M. Cavaletto[b], Jesús González-Vázquez[b], Alicia Palacios[b,c], and Fernando Martín[a,b,✉]

The Supplementary Information (SI) for the article "Advances in the Projected Forces and Momenta Decoherence Method for Attosecond Nonadiabatic Molecular Dynamics" contains: (i) additional explanations of the inactive-potential momentum propagation for the FM decoherence correction in presence of a laser field; (ii) additional figures and analysis for the ring-opening and ring-closing dynamics in the 1,2-dithiane molecule; (iii) the optimized ground-state geometries and harmonic frequencies used to build the Wigner distribution for all molecules.

[a] *Instituto Madrileño de Estudios Avanzados en Nanociencia (IMDEA-Nanociencia), Cantoblanco, 28049 Madrid, Spain.*
[b] *Departamento de Química, Módulo 13, Universidad Autónoma de Madrid, 28049 Madrid, Spain*
[c] *Condensed Matter Physics Center (IFIMAC), Universidad Autónoma de Madrid, 28049 Madrid, Spain.*
[†] *E-mail: gilbert.grell@imdea.org*
[✉] *E-mail: fernando.martin@uam.es*

S1 TSH-FM decoherence: Auxiliary momentum propagation with an explicit laser field

As outlined briefly in Sect. 2.2 of the main text, in the presence of a laser, the energy for a surface hop is understood to be absorbed from the field and the trajectory velocity is not adjusted to conserve energy if the hop occurs to a potential within the laser bandwidth[?] . For the FM decoherence correction, Eq. (5) of the main text, the inactive-potential population is interpreted as corresponding to wave packets traveling on auxiliary trajectories, defined in terms of their inactive-potential auxiliary forces and momenta, as detailed in Ref. [?] . An inactive-potential population increase is interpreted similar to a surface hop, i.e., requiring an energy-conserving correction in the field-free case but not in presence of an external field from which the necessary energy is absorbed. The energy-conserving auxiliary momentum propagation outlined in Section 2.6 of Ref. [?] , needs thus to be adapted as follows.

An inactive, i, (field-adiabatic) potential bearing a population above a threshold, η, is understood to harbor an auxiliary wave packet, the momentum of which has been propagated from the initial condition $P_i^f(0) = P_a^f(0) = P^f(0)$ at $t = 0$ according to the field-adiabatic force, $F_i^f(t)$. Sub-threshold populated potentials do not carry an auxiliary wave packet and the active-potential momentum is used.

$$P_i^f(t+\Delta t) = \begin{cases} P_i^f(t) + F_i^f(t)\Delta t, & |c_i^f(t)|^2 \geq \eta \quad \text{(S1)} \\ P_a^f(t+\Delta t), & |c_i^f(t)|^2 < \eta \quad \text{(S2)} \end{cases}$$

Here, the superscript f has been employed to indicate the field-adiabatic basis in presence of a laser field, see Sect. 2.2 of the main text. If the population of an inactive potential, i, falls below η during the propagation, its auxiliary wave packet has decohered and the remaining population is moved to the active potential, a, changing the momentum propagation from Eq. (**??**) to Eq. (**??**), effectively switching off decoherence, since $P_{ia}^f(t) = P_i^f(t) - P_a^f(t) = 0$ for these potentials, see Eq. (5) of the main text. If, in turn, the population of an inactive potential rises above η, it is interpreted as the birth of a new wave packet and the momentum propagation changes to Eq. (**??**). Finally, an increase of the inactive-potential population is interpreted as an excitation of a small wave packet from the active potential and the momentum propagation in Eq. (**??**) is modified by injecting active-potential momentum in proportion to the population increase, $\Delta\rho_{ii}^f(t) = \max\{0, |c_i^f(t)|^2 - |c_i^f(t-\Delta t)|^2\}$.

$$P_i^f(t) = P_i^f(t)\left(1 - \frac{\Delta\rho_{ii}^f(t)}{|c_i^f(t)|^2}\right) + \frac{\Delta\rho_{ii}^f(t)}{|c_i^f(t)|^2} P_a^f(t) \quad \text{(S3)}$$

S2 1,2-dithiane

Herein, additional data regarding the ring-opening dynamics in 1,2-dithiane is shown in Fig. **??**. The panels (a)-(c), respectively, depict for the TSH-PFM[?] , TSH-EDC[?] , and TSH-ND[?] approaches, the comparison of the adiabatic electronic populations, $\rho_{jj}(t)$, and fractions of active trajectories, $\Pi_j(t)$, for the S_0, S_1, and S_2 potentials in the sub-panels (a1)-(c1). While the TSH-PFM and TSH-EDC trajectory ensembles show almost perfect internal consistency, i.e., $\rho_{jj}(t) \approx \Pi_j(t)$, see Eq. (A.1) of Appendix A to the main text, TSH-ND violates internal consistency. After the first 50 fs, however, the TSH-ND fraction of active trajectories resembles the TSH-PFM and TSH-EDC values considerably better than the TSH-ND electronic populations. As the gradients and thus the nuclear dynamics are determined by the active potential, this explains why the TSH-ND simulation predicts almost the same structural dynamics as the TSH-PFM and TSH-EDC simulations, see Fig. 6 of the main text, although the TSH-ND electronic populations differ considerably from the TSH-PFM and TSH-EDC results. Panels (a2)-(c2) show the ensemble-averaged S_0, S_1, S_2 potential energy evolutions obtained with the respective methods. As expected from the aforementioned observation that the fraction of active trajectories is quite similar between all TSH approaches, the TSH-PFM, TSH-EDC, and TSH-ND average potential energies show only minute differences.

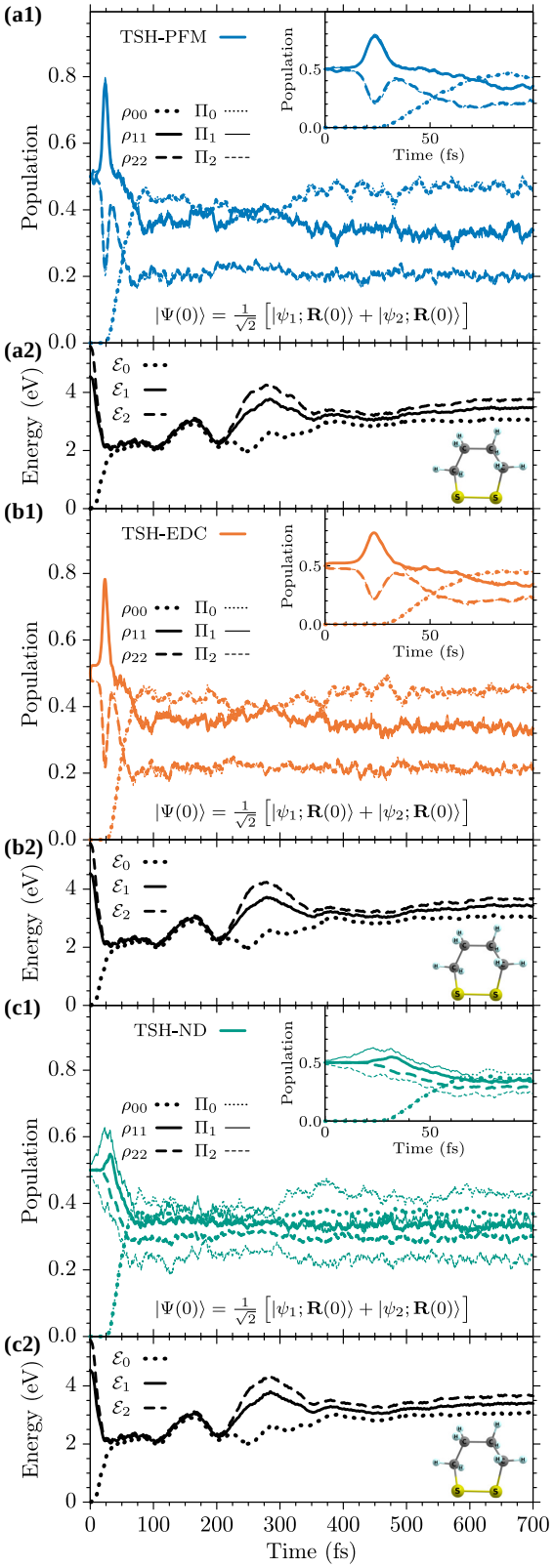

Fig. S1 Nonadiabatic dynamics in 1,2-dithiane after a 50:50 S_1-S_2 coherent superposition, $|\Psi(0)\rangle = \frac{1}{\sqrt{2}}[|\psi_1;\boldsymbol{R}(0)\rangle + |\psi_2;\boldsymbol{R}(0)\rangle]$. (a1) TSH-PFM adiabatic electronic populations, $\rho_{jj}(t)$ (thick), and fractions of active trajectories, $\Pi_j(t)$ (thin), for the S_0 (dotted), S_1 (solid), and S_2 (dashed), i.e., $j = 0, 1, 2$, adiabatic electronic potentials. (a2) TSH-PFM adiabatic S_0, S_1, and S_2 electronic potentials (black) using the same line styles as in (a1). (b1), (b2) same as (a1), (a2), but for TSH-EDC. (c1), (c2) same as (a1), (a2), but for TSH-ND. All TSH results have been obtained for respective ensembles of 1000 trajectories, see the main text.

S3 Molecular geometries and frequencies

S3.1 Lithium hydride

Optimized geometry of LiH, obtained as described in the main text. The bondlength is 3.158 a.u. (1.671 Å).

#	atom	x [a.u.]	y [a.u.]	z [a.u.]
1	Li	0.00000000E+00	0.00000000E+00	1.57880975E+00
2	H	0.00000000E+00	0.00000000E+00	-1.57880975E+00

Harmonic frequency of LiH, obtained as described in the main text.

mode	[cm^-1]	[eV]	[a.u.]
1	1.27078E+03	1.57556E-01	5.79009E-03

S3.2 Glycine

Optimized geometry of the I_p conformer of glycine, obtained as described in the main text, and in Ref. **?** .

#	atom	x [a.u.]	y [a.u.]	z [a.u.]
1	C	-2.14996201E-01	2.62921239E+00	6.63123794E-04
2	N	3.98901286E-01	-4.98748802E-02	7.45780415E-04
3	C	-3.02726220E+00	3.22335434E+00	7.78038040E-04
4	O	-3.45025189E+00	5.75216762E+00	7.38315997E-04
5	O	-4.70818622E+00	1.65803639E+00	6.94512145E-04
6	H	-5.28321740E+00	5.92653256E+00	7.54888895E-04
7	H	6.31754756E-01	3.56172806E+00	1.66292777E+00
8	H	6.31639729E-01	3.56159565E+00	-1.66173458E+00
9	H	-4.99920281E-01	-8.49347517E-01	-1.51460589E+00
10	H	-4.99631606E-01	-8.49183810E-01	1.51635457E+00

Harmonic normal mode frequencies of the I_p conformer of glycine, obtained as described in the main text, and in Ref. **?** .

mode	[cm^-1]	[eV]	[a.u.]
1	7.37532E+01	9.14423E-03	3.36044E-04
2	2.58736E+02	3.20792E-02	1.17889E-03
3	2.66285E+02	3.30151E-02	1.21328E-03
4	4.72463E+02	5.85780E-02	2.15270E-03
5	5.18476E+02	6.42828E-02	2.36235E-03
6	6.41123E+02	7.94891E-02	2.92117E-03
7	6.70373E+02	8.31156E-02	3.05444E-03
8	8.53511E+02	1.05822E-01	3.88888E-03
9	9.30071E+02	1.15314E-01	4.23771E-03
10	9.90731E+02	1.22835E-01	4.51410E-03
11	1.16341E+03	1.44244E-01	5.30088E-03
12	1.18686E+03	1.47152E-01	5.40774E-03
13	1.20277E+03	1.49125E-01	5.48023E-03
14	1.32638E+03	1.64450E-01	6.04343E-03
15	1.40467E+03	1.74157E-01	6.40013E-03
16	1.43436E+03	1.77838E-01	6.53542E-03
17	1.46568E+03	1.81721E-01	6.67814E-03
18	1.67288E+03	2.07410E-01	7.62219E-03
19	1.84797E+03	2.29119E-01	8.41995E-03
20	3.10734E+03	3.85261E-01	1.41581E-02
21	3.15915E+03	3.91685E-01	1.43942E-02
22	3.51392E+03	4.35670E-01	1.60106E-02
23	3.59606E+03	4.45855E-01	1.63849E-02
24	3.77639E+03	4.68212E-01	1.72065E-02

S3.3 1,2-Dithiane

Optimized geometry of 1,2-dithiane, obtained as described in the main text.

#	atom	x [a.u.]	y [a.u.]	z [a.u.]
1	S	-1.94146093E+00	5.11947821E-01	1.94056584E+00
2	S	1.94148330E+00	-5.11947361E-01	1.94054431E+00
3	C	2.83872502E+00	9.06955407E-01	-1.06372596E+00
4	C	-1.43214337E+00	2.24583539E-01	-3.32145528E+00
5	C	1.43210703E+00	-2.24583684E-01	-3.32147117E+00
6	C	-2.83873617E+00	-9.06955299E-01	-1.06369424E+00
7	H	-2.21481139E+00	-5.98205743E-01	-5.03354170E+00
8	H	-1.81397933E+00	2.23970159E+00	-3.40241744E+00
9	H	2.21475603E+00	5.98205350E-01	-5.03356640E+00
10	H	1.81394206E+00	-2.23970175E+00	-3.40243732E+00
11	H	-2.55373940E+00	-2.92955792E+00	-9.47166312E-01
12	H	-4.85083245E+00	-5.62762143E-01	-1.24002709E+00
13	H	2.55372956E+00	2.92955804E+00	-9.47195081E-01
14	H	4.85081933E+00	5.62762219E-01	-1.24008122E+00

Harmonic normal mode frequencies of 1,2-dithiane obtained as described in the main text.

mode	[cm^-1]	[eV]	[a.u.]
1	1.79074E+02	2.22023E-02	8.15919E-04
2	2.32990E+02	2.88871E-02	1.06158E-03
3	3.12474E+02	3.87419E-02	1.42374E-03
4	3.57356E+02	4.43065E-02	1.62823E-03
5	3.93085E+02	4.87364E-02	1.79103E-03
6	4.59064E+02	5.69167E-02	2.09165E-03
7	5.28013E+02	6.54653E-02	2.40580E-03
8	7.17255E+02	8.89283E-02	3.26805E-03
9	7.24709E+02	8.98525E-02	3.30202E-03
10	8.65891E+02	1.07357E-01	3.94529E-03
11	9.10956E+02	1.12944E-01	4.15062E-03
12	9.65170E+02	1.19666E-01	4.39764E-03
13	1.01465E+03	1.25801E-01	4.62310E-03
14	1.06595E+03	1.32161E-01	4.85681E-03
15	1.14516E+03	1.41982E-01	5.21774E-03
16	1.17144E+03	1.45240E-01	5.33749E-03
17	1.23940E+03	1.53666E-01	5.64710E-03
18	1.30103E+03	1.61307E-01	5.92792E-03
19	1.38072E+03	1.71188E-01	6.29104E-03
20	1.39375E+03	1.72803E-01	6.35039E-03
21	1.45720E+03	1.80669E-01	6.63948E-03
22	1.47390E+03	1.82741E-01	6.71560E-03
23	1.52035E+03	1.88499E-01	6.92720E-03
24	1.54035E+03	1.90979E-01	7.01834E-03
25	1.60667E+03	1.99202E-01	7.32053E-03
26	1.61110E+03	1.99751E-01	7.34070E-03
27	1.62638E+03	2.01645E-01	7.41031E-03
28	1.63813E+03	2.03102E-01	7.46387E-03
29	3.19337E+03	3.95927E-01	1.45501E-02
30	3.20797E+03	3.97738E-01	1.46166E-02
31	3.23036E+03	4.00514E-01	1.47186E-02
32	3.23618E+03	4.01235E-01	1.47451E-02
33	3.24236E+03	4.02002E-01	1.47733E-02
34	3.24930E+03	4.02863E-01	1.48049E-02
35	3.29261E+03	4.08232E-01	1.50022E-02
36	3.29334E+03	4.08322E-01	1.50056E-02

Notes and references

M. Richter, P. Marquetand, J. González-Vázquez, I. Sola and L. González, *J. Chem. Theory Comput.*, 2011, **7**, 1253–1258.

G. Grell, J. González-Vázquez, F. Fernández-Villoria, A. Palacios and F. Martín, *J. Chem. Theory Comput.*, 2025, **21**, 10645–10668.

G. Granucci and M. Persico, *J. Chem. Phys.*, 2007, **126**, 134114.

J. C. Tully, *J. Chem. Phys.*, 1990, **93**, 1061–1071.

J. Galiana, S. M. Cavaletto, G. Grell, F. Fernández-Villoria, A. Palacios, J. González-Vázquez and F. Martín, *J. Chem. Theory Comput.*, 2026, **22**, 1224–1243.